www.czasopisma.pan.pl PAN POLSKA AKADEMIA NAUK www.journals.pan.pl

A R C H I V E S O F M E T A L L U R G Y A N D M A T E R I A L S

Volume 58 2013 Issue 2

DOI: 10.2478/v10172-012-0196-z

A. SYPIEŃ*

OBSERVATION OF THE COMPLEX LOCAL CRYSTALLIZATION PROCESS IN Ti-Zr-Cu-Pd AMORPHOUS RIBBONS AND BULK METALLIC GLASS

CHARAKTERYSTYKA PROCESU LOKALNEJ KRYSTALIZACJI W AMORFICZNYCH TAŚMACH I MASYWNYCH SZKŁACH METALICZNYCH Ti-Zr-Cu-Pd

In recent years, bulk metallic glasses (BMGs) have attracted much attention, especially concerning the reasons for the high glass-forming ability. To understand properties and glass-forming ability of BMGs, it is important to investigate their atomic structure in details. The structure of the metallic glass, derived from diffraction studies, confines mainly to short-range-order atomic correlations, which are statistically averaged over the glassy specimens. In the present study, local structure of a BMG and ribbons was observed using a high-resolution TEM (TECNAI G^2 FEG). The TEM images of the BMG before annealed in the temperature below the crystallization clearly reveal a duplex microstructure consisting of nanocrystalline particles about 5-10 nm in size distributed uniformly in the amorphous matrix. Due to the FFT research the crystalline phases may be indexed as the Cu_8Zr_3, Cu_3Pd, $CuTi_2$ and CuTiZr.

Keywords: ribbons, bulk metallic glass, TEM, HREM, primary crystallization

W ostatnich latach dużym zainteresowaniem cieszy się poszukiwanie składów stopów, które charakteryzuje wysoka zdolność do tworzenia faz amorficznych, a co za tym idzie, tworzenia masywnych szkieł metalicznych. Aby zrozumieć właściwości oraz zdolność materiału metalicznego do zeszklenia należy zbadać szczegółowo jego strukturę atomową. Badania dyfrakcyjne metali amorficznych pozwalają jedynie na uzyskanie informacji na temat uporządkowania bliskiego zasięgu. Niniejsza praca przedstawia bardziej wnikliwe badania lokalnej struktury szkieł metalicznych, które uzyskano przy użyciu transmisyjnej mikroskopii elektronowej TEM. Wybrany stop o składzie $Ti_{40}Zr_{10}Cu_{40}Pd_{10}$ został poddany wygrzewaniu w temperaturze poniżej temperatury krystalizacji. Badania HREM ujawniły, iż powstała w materiale mikrostruktura składała się z nanocząstek o wielkości około 5-10nm w amorficznej osnowie. Analizy składu chemicznego EDX oraz obrazów transformaty Fouriera wskazują, iż krystaliczne fazy mogą być zidentyfikowane jako Cu_8Zr_3, Cu_3Pd, $CuTi_2$ i CuTiZr.

1. Introduction

Various medical metallic materials have been developed on the basis of the unique characteristics of titanium. In case of bone injury, recovery techniques for surgical reduction of bone fragments require fixtures and stems of various shapes [1, 2]. Typical metallic biomaterials such as Ti-6Al-4V alloy, stainless steel and Co-based alloys still pose a potential hazard due to the addition of toxic elements, low physical durability and chemical stability in a human body. Glassy type structural alloys can be regarded as new biomaterials because of useful engineering properties such as high strength and good corrosion resistance, which cannot be obtained for crystalline alloys [3]. Recently, investigations report on development of Ti-Zr-Cu-Pd bulk glassy alloy system with critical diameters of 6-7 mm [4, 5]. BMGs from this system can exhibit a yield strength as high as 2000 MPa and good corrosion resistance without the addition of Be and Ni elements which are hazardous for human health. Therefore, the development of a new Ti-based BMG on the basis of this concept may bring forth a novel and promising type of biomaterial.

2. Experimental procedure

Master alloy with nominal composition of $Ti_{40}Zr_{10}Cu_{40}Pd_{10}$ (named "base alloy", numbers indicate at.%) was prepared by cold crucible levitation melting from high purity elements (99.99 wt.%) in an argon atmosphere [6]. From this master alloy, cast cylinders of 3 mm in diameter and 45 mm in length were obtained by injection casting into a copper mold in a purified argon atmosphere. The ribbon samples with a thickness of 20 μm and 5 mm of width were prepared by melt spinning on a single copper roller at a linear speed of 40 m/s. Phase transformations were studied by differential scanning calorimetry (DSC Q1000, TA Instruments) at a heating rate of 20 K/min and by isothermal calorimetry in an argon protective atmosphere. Samples were prepared after annealing both the BMG and the ribbon in the temperature

* POLISH ACADEMY OF SCIENCES, INSTITUTE OF METALLURGY AND MATERIALS SCIENCE, 30-059 KRAKOW, POLAND

of the firs crystallization peak observed on the DSC curve. The annealing process of the ribbon was conducted in two steps: 430°C for 3 minutes and at 436°C for 1 minute. The bulk metallic glass was annealed in one step at 431°C for 3 minutes.

In the present study, local structure of BMG and ribbon was observed using a high-resolution TEM (FEI, TECNAI G^2 FEG with acceleration voltage of 200kV). Thin foils for HREM were prepared by electropolishing and additionally thinned with the ion gentle milling system (Technoorg Linda).

3. Results and discussion

In order to understand the nature of the metastable phase forming at the first stage of crystallization, the amorphous alloy was heated in the DSC at 20 K/min to the first crystallization peak temperature and then cooled rapidly.

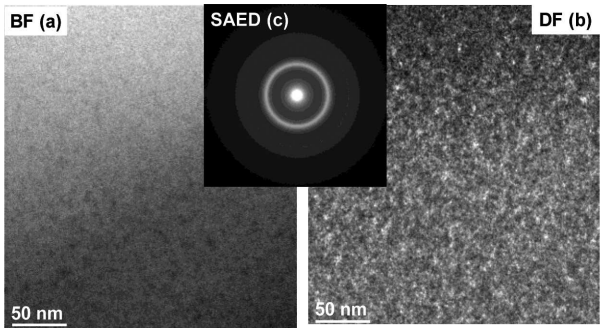

Fig. 1. TEM bright – field (BF) image (a), dark field (DF) image (b) and selected area electron diffraction pattern (SAED) (c) of the $Ti_{40}Zr_{10}Cu_{40}Pd_{10}$ ribbon annealed at 430°C for 3 min

The ribbon samples were annealed in the temperature of the first exothermic peak in two steps. In the first step the samples were annealed at 430°C for 3 minutes. Fig. 1 and Fig. 2 show the typical transmission electron microscope (TEM) and high-resolution TEM (HREM) microstructures obtained from the amorphous sample. The HREM (Fig. 2a) and the corresponding Selected Area Electron Diffraction Pattern (SAEDP), (Fig. 1c) with a diffused halo, indicate a uniform amorphous microstructure. These results reveal that the alloy annealed at 430°C for 3 min contains no crystalline particles. The first nanocrystallites were detected after the second step. In the second step, the samples were annealed at 436°C for 1min (Fig. 3, Fig. 4). Fig. 3a presents local areas with nanocrystalline inclusions surrounded by the amorphous matrix. The microstructure in Bright Field (BF) mode in Fig. 3b presents the zone with some inclusions seen as dark particles. The same area is shown in Fig. 3c were small bright particles indicate the presence of nanocrystallites. The selected area electron diffraction pattern (Fig. 3d) shows some diffraction spots forming thin rings superimposed on the diffused halo. These results confirm the amorphous-nanocrystalline structure of the material. The HREM images (Fig. 4a) clearly show the crystallized regions which are surrounded by the amorphous phase. Fig. 4c presents the Fast Fourier Transform (FFT) image from the area marked in Fig. 4a. The reflections indicate the presence of α-Cu_3Pd phase in [001] zone axis orientation. Amorphous regions with Short Range Ordering (SRO) contrast are observed between the crystals. The size of these amorphous zones ranges between 4-6 nm. The Inversed Fast Fourier Transform (IFFT) image in Fig. 4b presents the same area as in Fig. 4a. The zone marked with white ellipses consists of crystallites with the atomic plane spacing about 0.2 nm.

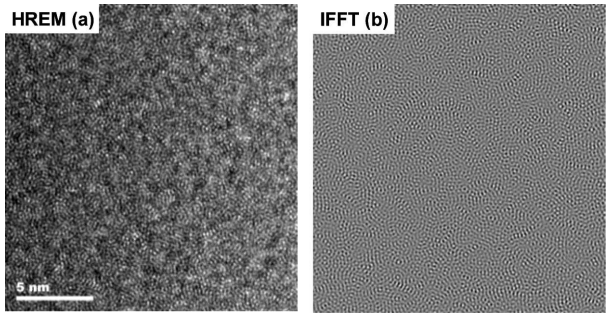

Fig. 2. HREM image showing the amorphous structure of the alloy annealed at 430°C for 3 min (a) and the corresponding IFFT image (b)

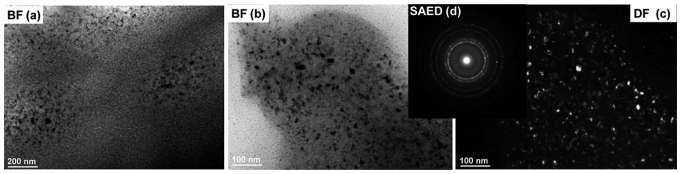

Fig. 3. TEM BF images (a), (b), DF image (c) and SAED pattern (d) of the $Ti_{40}Zr_{10}Cu_{40}Pd_{10}$ ribbon annealed in two steps: 1 – at 430°C for 3 min, 2 – at 436°C for 1 min

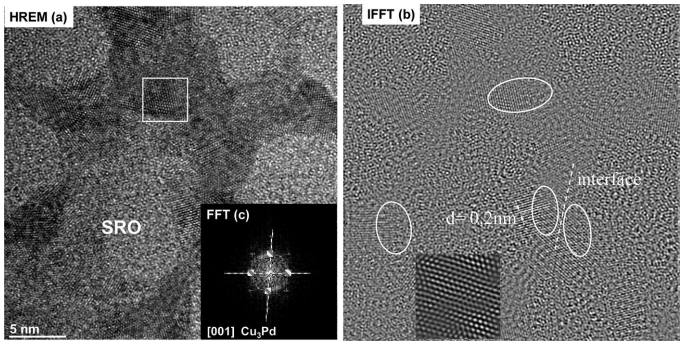

Fig. 4. HREM image, showing the occurrence of nanocrystallization of the alloy annealed in two steps: 1 – at 430°C for 3 min, 2 – at 436°C for 1min and the corresponding IFFT image with white ellipses on the image denoting areas of long range ordering

The bulk metallic glass samples were annealed in the temperature of the first exothermic peak in one step at 431°C for 3 minutes. Fig. 5, 6, 7 revealed a duplex microstructure consisting of nanocrystalline particles of about 5-10 nm in size distributed uniformly in the amorphous matrix. The chemical composition analyses performed by energy dispersive spectroscopy (EDS) at the two points and areas marked as “1” and ”2” in Fig. 6(a, b) reveal that the dark phase is enriched in titanium whereas bright phase contains less titanium and more copper. The EDX line scan investigation with TEM technique confirmed this conclusion (Fig. 6c).

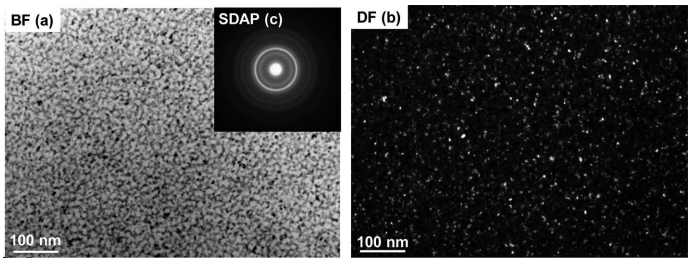

Fig. 5. TEM BF images (a), (b), DF image (c) and SAED pattern (d) of the $Ti_{40}Zr_{10}Cu_{40}Pd_{10}$ bulk metallic glass annealed at 431°C for 3 min

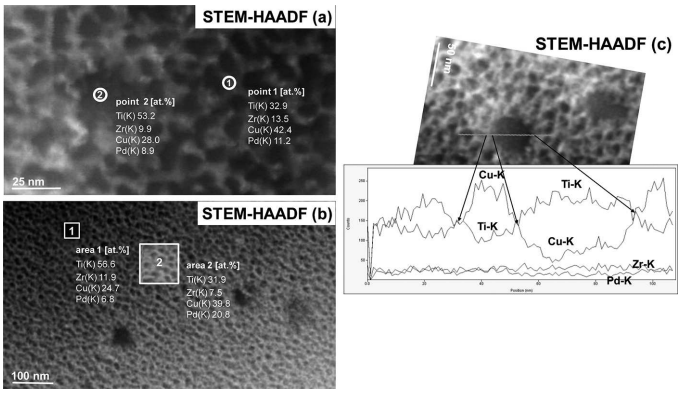

Fig. 6. (a), (b), (c) STEM-HAADF images of the $Ti_{40}Zr_{10}Cu_{40}Pd_{10}$ BMG annealed at 431°C for 3 min with the points and areas of chemical composition analyses (at.%) as well as (d) corresponding EDX line scan

Although crystalline atomic clusters are as small as 1-2 nm, the FFT pattern of a single cluster could be obtained. The nanocrystallites were identified as three different phases (Fig. 7): the orthorhombic Cu_8Zr_3 in [021] and [111] zone axes, (space group Pmcn, a=0.814 nm, b=0.997 nm, c= 0.786 nm), tetragonal $CuTi_2$ in [331] zone axis, (space group I4/mmm, a=0.294 nm, c= 0.107 nm) and tetragonal Cu_3Pd in [001] zone axis, (space group P4 mm, a=0.371 nm, c= 2.565 nm).

The study of the crystallization process showed that in the range of the first thermal effect the phase precipitating as crystallites is a metastable solid solution. The primary crystallization process generates the concentration gradient of the elements what subsequently leads to the diffusion in the crystallites. Then, the crystal growth is controlled by the long range order diffusion. In the case of metal-non-metal glasses, the diffusion of non-metallic atoms is a limiting factor for the primary crystals growth because of the phenomena occurring at the interphase. The crystallization in Ti-Zr-Cu-Pd alloys occurs by diffusion of Ti and Cu atoms between amorphous and crystalline regions. This effect can be explained assuming the existence of small quenched-in clusters with short-range order located close to a crystalline phase, which can serve as nuclei or sites for heterogeneous nucleation of crystals. This result confirms the previous report by Inoue et al.[7], wherein they suggested the presence of a minor fraction of amorphous phase along with a large fraction of the first phase obtained by primary crystallization of this alloy.

4. Conclusions

1. the detailed investigation of the first stage of crystallization of the Ti-Zr-Cu-Pd amorphous alloy shows that the glass-crystal transformation occurs gradually by the formation of a number of intermediate metastable phases. The increasing of the annealing temperature leads, initially to the increase of the ordering in the microareas (Fig. 2) and then to the growth of nanocrystals of the metallic element distributed uniformly in the amorphous matrix (Fig. 4, Fig. 7).

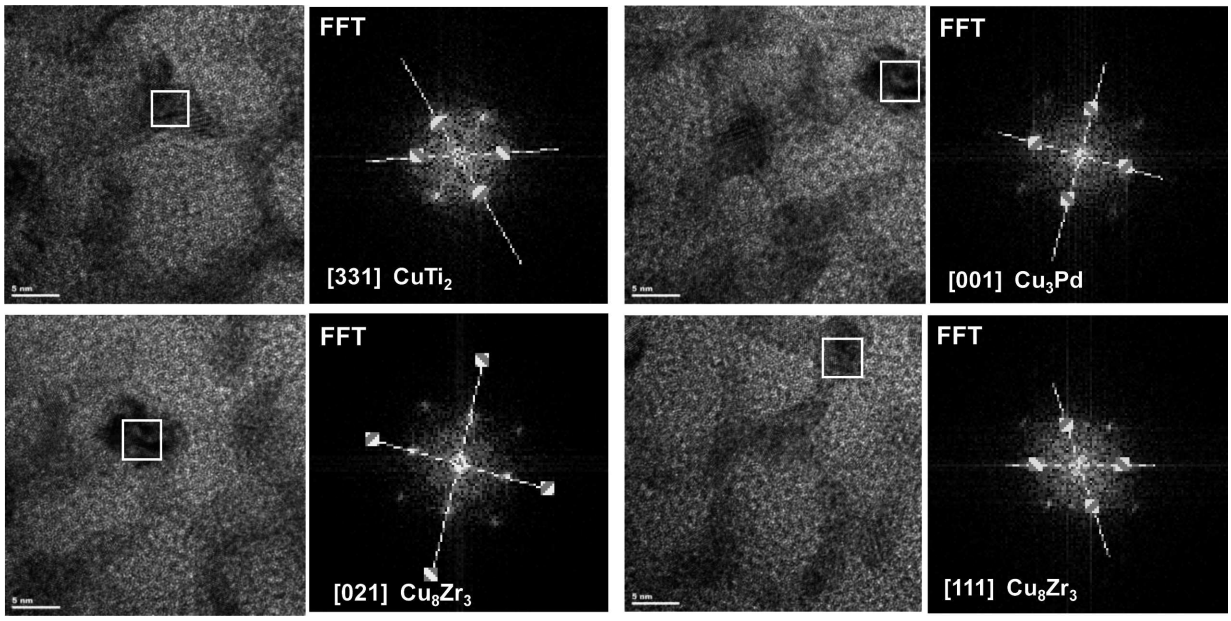

Fig. 7. HREM images showing the occurrence of nanocrystallization and Fast Fourier Transform (FFT) patterns from the areas marked with white squares

2. the annealing of both the ribbon and the BMG leads to the formation of nanocrystalline particles about 5-10 nm in size.
3. the detected nanocrystals are enriched in Cu in comparison with the matrix. Although crystalline atomic clusters are as small as 1-2 nm, they can be clearly imaged, even embedded in the amorphous phase.
4. the FFT research allowed the index the crystalline phases as the Cu_8Zr_3, $CuTi_2$, Cu_3Pd and CuTiZr.

Acknowledgements

Research was financially supported by the Ministry of Science and Higher Education in Poland under the Grant No. 3039/B/T02/2011/40. The studies were performed in the Accredited Testing Laboratories at the Institute of Metallurgy and Materials Science of the Polish Academy of Sciences.

Received: 20 January 2013.

REFERENCES

[1] D.C. Meyer, L.E. Ramseier, G. Lajtai, H. Nötzli, Clin. Biomechan. **18**, 975 (2003).
[2] P. Korovessis, D. Deligianni, G. Petsinis, A. Baikousis, Eur. J., Orthop. Surg. Traumatol. **12**, 61 (2002).
[3] S. Hiromoto, K. Asami, A.-P. Tsai, M. Sumita, T. Hanawa, Corros., Sci. **43**, 1767 (2001).
[4] S.L. Zhu, X.M. Wang, F.X. Qin, A. Inoue, Mater Sci. Eng A **459**, 233-237 (2007).
[5] S.L. Zhu, X.M. Wang, F.X. Qin, M. Yoshimura, A. Inoue, Mater Trans **48**, 2445-2448 (2007).
[6] A. Sypień, W. Przybyło, Materials Science and Technology **26**, 1, 31-35 (2010).
[7] A. Inoue, T. Zhang, J. Saida at all, Mater. Trans. JIM. **40**, 1137 (1999).